2

UED THEORY*

2.1 Introduction

The general theory of GED is well-established;[1, 2] here, we summarize the basic equations used in the analysis of scattering patterns and the subsequent extraction of internuclear separations. Electron scattering intensity is typically expressed as a function of *s*, the magnitude of momentum transfer between an incident electron and an elastically scattered electron:

$$s = \frac{4\pi}{\lambda}\sin\left(\frac{\theta}{2}\right) \qquad (2\text{–}1)$$

---

* Parts of this chapter have been adapted from Srinivasan, R.; Lobastov, V.A.; Ruan, C.-Y.; Zewail, A.H., *Helv. Chim. Acta*, **2003**, *86*, 1762.

where λ is the de Broglie wavelength of the electrons (0.067 Å at 30 keV) and θ is the scattering angle.

The total scattering intensity, I, is a sum of contributions from individual atoms (atomic scattering, I_A) superimposed with interference terms from all atom–atom pairs (molecular scattering, I_M):

$$I(s) = I_A(s) + I_M(s) \tag{2–2}$$

In the independent-atom model, where the independence of the electronic potentials of each atom in the molecule is assumed, the atomic scattering intensity can be written as a sum of elastic and inelastic scattering contributions:

$$I_A(s) = C\sum_{i=1}^{N}\left(\left|f_i(s)\right|^2 + 4\frac{S_i(s)}{a_0{}^2 s^4}\right) \tag{2–3}$$

where N is the number of atoms in the molecule; f_i and S_i are, respectively, the elastic and inelastic scattering amplitudes for atom i, respectively; a_0 is the Bohr radius; and C is a proportionality constant. The contributions from spin-flip scattering amplitudes (g_i) have not been included as they are generally neglected for high-energy electron diffraction experiments.[3]

For the purpose of structural determination, only I_M is of interest because it contains the information regarding internuclear separations. The molecular scattering intensity of an isotropic sample can be written as a double sum over all N atoms in the molecule:

$$I_M(s) = C\sum_{i}^{N}\sum_{j\neq i}^{N}|f_i||f_j|\exp\left(-\frac{1}{2}l_{ij}^{\,2}s^2\right)\cos(\eta_i-\eta_j)\frac{\sin(sr_{ij})}{sr_{ij}} \qquad (2\text{–}4)$$

where f_i is the elastic scattering amplitude for the ith atom, η_i is the corresponding phase term, r_{ij} is the internuclear separation between atoms i and j, l_{ij} is the corresponding mean amplitude of vibration, and C is a proportionality constant. The atomic scattering factors f and η depend on s and atomic number Z; tables of f and η are available in the literature[4] with f scaling as Z/s^2 (*Rutherford* scattering). The relative contribution of each atomic pair to the total molecular scattering intensity (from Eqn. 2–4) is, therefore, roughly proportional to $(Z_iZ_j)/r_{ij}$. Since $I_M(s)$ decays approximately as s^{-5}, the modified molecular scattering intensity, $sM(s)$, is often used instead of $I_M(s)$ in order to highlight the oscillatory behavior $(\sin(sr_{ij})/r_{ij})$ of the diffraction signal at higher values of s; note that the $\sim s^{-5}$ dependence arises from the s^{-2} contribution from f_i and similarly from f_j, along with the $1/s$ term of the sinc function, which results from isotropic averaging in the gas sample.

The modified molecular scattering intensity can be defined either as:

$$sM(s) = s\frac{I_{\mathrm{M}}(s)}{I_{\mathrm{A}}(s)} \tag{2–5a}$$

or

$$sM(s) = s\frac{I_{\mathrm{M}}(s)}{|f_a||f_b|} \tag{2–5b}$$

where a and b correspond to two chosen atoms in the molecule (usually atoms with relatively high Z). Note that the experimental $I_{\mathrm{M}}{}^{E}(s)$ can be transformed into $sM^{E}(s)$ by simply dividing by an atomic reference signal (xenon gas, in our case) and multiplying by s (obtained from measured θ through the known camera length).

Although the molecular scattering function contains all of the structural information about the molecule, a more intuitive interpretation of experimental results is achieved by taking the Fourier (sine) transform of $sM(s)$ and examining $f(r)$, the radial distribution function:

$$f(r) = \int_0^{s_{\max}} sM(s)\sin(sr)\exp\left(-ks^2\right)ds \tag{2–6}$$

where k is a damping constant. The exponential damping term filters out the artificial high frequency oscillations in $f(r)$ caused by the cutoff at $s_{\max}$. The radial distribution curve reflects the relative density of internuclear distances

in the molecule. In our UED-3 experiments, the available experimental scattering intensity, $sM^E(s)$, typically ranges from s_{min} = 1.5 Å^{-1} to s_{max} = 18.5 Å^{-1} (θ from 0.9° to 11.3°). For the range from 0 to s_{min}, the theoretical scattering intensity, $sM^T(s)$, is appended to avoid distortions of the radial distribution baseline. It should be noted that all data analyses and structural refinements are performed on $sM^E(s)$ and not $f(r)$ because of inaccuracies that could potentially be introduced into $f(r)$ through improper choice of k.

2.2 The Diffraction-Difference Method: Transient Structures

To follow the structural changes that occur over the course of a given reaction, a series of averaged 2D diffraction images are recorded—with varying time delay, t (see Fig. 2–1). Before analyzing the time-dependent diffraction signals, we normalize the intensity of each time-dependent 2D image to the total number of electrons detected on the CCD. This normalization procedure accounts for any systematic variation (1% or less) in electron scattering intensity as a function of temporal delay. Each of these normalized, averaged images, thus, reflects the transient behavior of the molecular structures at a particular temporal delay following excitation. Unlike the ground-state data, the scattering intensity at time $t > 0$, $I(t > 0; s)$, contains contributions from more than one type of molecular species—not just the reactant structures, but also the transient, intermediate, and product

structures of the reaction.

Structural dynamics of a species involves two important changes: *population* change and *structural* change. Consider the following reaction:

$$S_R \rightarrow S_I \rightarrow S_P \tag{2–7}$$

where there is a change of species from reactant (S_R) through intermediate (S_I) to product (S_P). A species is defined as a molecular entity with a particular chemical formula. The time-resolved scattering intensity $I(t; s)$ can be written as a sum of the individual scattering intensities from each species, $I_\alpha(t; s)$, at time t:

$$I(t;s) = \sum_\alpha I_\alpha(t;s) = \sum_\alpha p_\alpha(t) \cdot \sigma_\alpha(t;s) \tag{2–8}$$

where α indexes all possible species (reactant, intermediate, or product) occurring over the course of the reaction, $p_\alpha(t)$ is the normalized probability, henceforth referred to as the population of a given species, α, and $\sigma_\alpha(t; s)$ is the effective scattering cross-section from that species. Depending on the time resolution of the diffraction experiment, we can resolve either the temporal change in species population, $p_\alpha(t)$, or the temporal change in species structure—manifested as a change in the effective scattering cross-section,

$\sigma_\alpha(t; s)$—or both.

In UED, all species present will scatter the incident electrons regardless of their participation in the reaction. Thus, in most cases, the vast majority (>85–90%) of the diffracting media is comprised of non-reacting parent molecules: $p_{\text{reactant}} >> p_{\text{intermediate}}$ or p_{product}. Furthermore, the molecular scattering intensity from a reaction fragment is usually weaker than that from the parent molecule because it has fewer internuclear pairs. Therefore, to accentuate the diffraction signal arising from structural changes occurring over the course of the reaction, we employ the diffraction-difference method,[5] wherein we use a reference image to obtain the diffraction-difference signal, $\Delta I(t; t_{\text{ref}}; s)$, from the relation:

$$\Delta I(t; t_{\text{ref}}; s) = I(t; s) - I(t_{\text{ref}}; s) \tag{2–9}$$

where t_{ref} refers to the reference time (e.g., prior to the arrival of the reaction-initiating laser pulse). Combining Eqns. 2–8 and 2–9 gives

$$\Delta I(t; t_{\text{ref}}; s) = \sum_\alpha p_\alpha(t) \cdot \sigma_\alpha(t; s) - \sum_\alpha p_\alpha(t_{\text{ref}}) \cdot \sigma_\alpha(t_{\text{ref}}; s) \tag{2–10}$$

The experimental diffraction intensity curve is a sum of the desired structural information, $I_M^E(s)$, and a background intensity profile, $I_B^E(s)$:

$$I^E(s) = I_B{}^E(s) + I_M{}^E(s) \tag{2–11}$$

where $I_B{}^E(s)$ contains contributions from atomic scattering, $I_A(s)$, and the experimental background response. It follows from this definition that the experimental difference curve is given by:

$$\Delta I^E(t; t_{ref}; s) = \Delta I_M{}^E(t; t_{ref}; s) + \Delta I_B{}^E(t; t_{ref}; s) \tag{2–12}$$

Because $I_B{}^E$ is comprised mostly of atomic scattering, which is unchanged over the course of a chemical reaction, $\Delta I_B{}^E(t; t_{ref}; s)$ should be nearly zero. Thus, whereas the total diffraction signal, $I(t; s)$, is dominated by the background intensity, $I_B{}^E(t; s)$, the diffraction-difference curve is dominated by the molecular scattering intensity, $I_M{}^E(t; s)$:

$$\Delta I^E(t; t_{ref}; s) \approx \Delta I_M{}^E(t; t_{ref}; s) \tag{2–13}$$

Thus, Eqn. 2–13, which is a direct consequence of the diffraction-difference approach, allows us to obtain transient molecular structures even if their population is small relative to the unchanging background (Fig. 2–2). It may be noted that the diffraction-difference method does not depend on the

specific formulae used to express I_M. While the well-known description, Eqn. 2–4, is usually used, formulae more sophisticated than Eqn. 2–4 have been used in our UED studies.

One of the most important features of the diffraction-difference method is the control over t_{ref}. The choice of t_{ref}—the sequence of the electron pulses—allows us to isolate structures of different species evolving with time:

(1) By choosing t_{ref} to be at negative time, we can obtain the ground-state diffraction pattern. Also, by recording diffraction images at two different negative times (probing the same reactant structure at each of these times), we can obtain a control diffraction-difference image to verify the absence of rings.

(2) By choosing t_{ref} to be at a specific positive time, we can isolate different transient species in, say, non-concerted reactions based on the relevant timescales of the non-concerted bond breaking, as described for the case of $C_2F_4I_2$ in Chapter 5 (see Fig. 2–3).

(3) Finally, we can also extract the molecular diffraction signal resulting only from the transient species via the 'transient-only' or the 'transient-isolated' method. In this case, the reactant diffraction signal ($I_{reactant}(s)$, obtained at a negative time) is scaled by the fractional change, $\Delta p_{reactant}(t;\ t_{ref})$, and added to the diffraction difference signals obtained at positive times, thereby canceling out the parent contribution:

$$\Delta I(t;t_{\text{ref}};s) + \Delta p_{\text{reactant}}(t;t_{\text{ref}}) \cdot I_{\text{reactant}}(s) = \sum_{\alpha \neq \text{reactant}} \Delta p_{\alpha}(t;t_{\text{ref}}) \cdot \sigma_{\alpha}(t;s) \qquad (2\text{–}14)$$

2.3 Ground-State Structures

Ground-state diffraction patterns are obtained by timing the electron pulse to arrive at the molecular sample before the laser pulse (negative time; see Fig. 2–1) or by completely blocking the laser arm (to reduce the noise due to laser light). From Eqn. 2–5, the modified experimental molecular scattering intensity of the ground-state is given by:

$$sM^{E}(s) = s\frac{I^{E}(s) - I_{\text{B}}{}^{E}(s)}{I_{\text{A}}(s)} \qquad (2\text{–}15a)$$

or

$$sM^{E}(s) = s\frac{I^{E}(s) - I_{\text{B}}{}^{E}(s)}{|f_a||f_b|} \qquad (2\text{–}15b)$$

We do not obtain the curve for $I_{\text{B}}{}^{E}(s)$ by merely calibrating the detector because the amount of scattered laser light and other factors vary from experiment to experiment and with each molecular system. Instead, background curves are independently obtained for each experiment. Such background curves may be ascertained by different methods, three of which

are described: (1) A crude yet often effective approximation is a low-order polynomial curve fit through all the data points of $I^E(s)$; (2) A more rigorous way of obtaining $I_B{}^E(s)$ exploits the sinusoidal nature of $I_M(s)$, cycling above and below zero several times over the experimental detection range. This approach introduces a set of zero-positions, s_n, of s where the theoretical molecular intensity curve, $I_M{}^T(s)$, crosses zero, *i.e.*, $I_M{}^T(s_n) = 0$. If $I_M{}^T(s)$ approaches $I_M{}^E(s)$, it should then hold from Eqn. 2–2 that $I^E(s_n) = I_B{}^E(s_n)$ at the zero-positions, s_n. Therefore, $I_B{}^E(s)$ can be approximated by fitting a polynomial curve through $[s_n, I^E(s_n)]$; (3) A third way to obtain $I_B{}^E(s)$ is to express $I_B{}^E(s)$ independently as a polynomial curve defined by the variable coefficients of each order, and to optimize these variables by minimizing the difference (more precisely, χ^2) between $I_M{}^T(s)$ and $I_M{}^E(s)$. This method should produce the same background curve obtained with the second method if there is no systematic error. The three methods can also be applied to the time-resolved diffraction data. Currently, method (3) as described above is the method of choice in UED-3.

2.4 Structure Search and Refinement

UED utilizes quantum-chemical calculations as a starting point for the global conformational search. In UED-3, the structure parameters are constructed with internal coordinates of a geometrically consistent structural

model for the molecule—the so-called *Z*-matrix of quantum chemistry—to facilitate easier comparison between theory and experiment. To ensure that all possible structures are considered in the refinements, Monte Carlo sampling procedures are applied to search all possible good fits to the data (in terms of χ^2) in a configuration space set up by the *Z*-matrix coordinates. The distance between any two given structures is defined as the square root of the sum of the squared displacements between all corresponding nuclear coordinates of the two structures. Based on the distance between randomly sampled structures to a starting structure, the configuration hyperspace is first partitioned and then searched for local minima. When the sampling within the partitioned subspace is found to converge to a local χ^2 minimum, the radius of convergence is determined along each adjustable internal coordinate to give the size of local minimum basin. Finally, lowest-local-minima structures are statistically analyzed to reveal the ensemble distribution of a global minimum structure. The Monte Carlo sampling algorithm, coupled with the internal coordinate representation, allows the fit structure to be vastly different from the starting model provided by quantum calculations. This forms the basis of the UED-3 structural search in large conformational space guided by experiment.

Refinement of the diffraction data is performed with software developed in our laboratory at Caltech using a procedure that iteratively

minimizes the statistical χ^2. For example, for a given difference curve, $\Delta I^E(t; t_{ref}; s)$, the determination of the relative fractions or structural parameters of each molecular species is made by minimizing

$$\chi^2 = \sum_{s_{min}}^{s_{max}} \frac{[S_c \cdot \Delta sM^T(t; t_{ref}; s) - \Delta sM^E(t; t_{ref}; s)]^2}{[\delta(s)]^2} \qquad (2\text{–}16)$$

where the $\Delta sM(s)$ is the difference-modified molecular-scattering intensity, $\delta(s)$ is the standard deviation of $\Delta sM^E(t; t_{ref}; s)$ at each s position (over the available range), and S_c is a scaling factor (whose magnitude is determined by the amplitude of the ground-state signal). $\Delta sM^E(t; t_{ref}; s)$ is obtained from $\Delta I^E(t; t_{ref}; s)$ by Eqn. 2–15, and the $\delta(s)$ values are calculated from the corresponding values of $\delta(pix)$ (the standard deviation of the scattering intensity at each pixel radius) with appropriate error propagation.

Beginning with an assumed initial species distribution and the starting structural parameters for each species, the software first fits the residual background, $\Delta I_B^E(t; t_{ref}; s)$, as a polynomial curve by optimizing the variable coefficients in order to minimize the difference (more precisely, χ^2) between $I_M^T(s)$ and $I_M^E(s)$. Then the experimental $\Delta sM^E(t; t_{ref}; s)$ curve is obtained with the background-free ΔI by Eqn. 2–15, and χ^2 is calculated to evaluate the quality of the fit. This procedure is repeated until the best least-

squares fit between theoretical and experimental $\Delta sM(s)$ curves is reached (*i.e.*, until χ^2 is minimized).

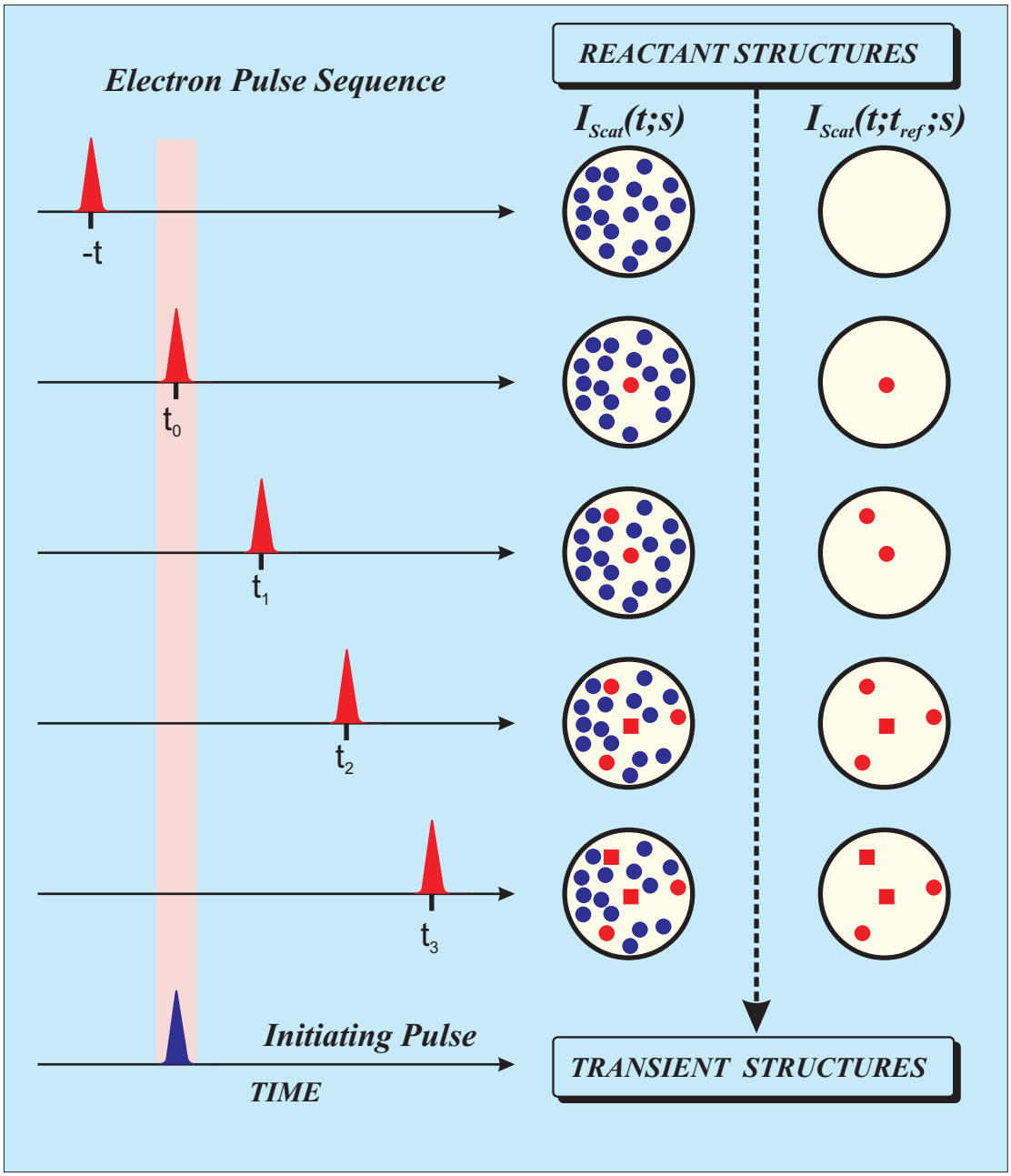

Figure 2-1. Concept of Ultrafast Electron Diffraction. An ultrafast initiation pulse (*shown in blue*) triggers the reaction and a second ultrashort electron pulse (*shown in red*) probes the resulting structural change. The electron pulse can be timed to arrive before the initiating pulse (*negative time*) thus probing the parent (*shown as blue filled circles*) or after the laser pulse (*positive time*), now probing the transient structures also (*shown as red filled circles and squares*). The time at which the light and electron pulses arrive simultaneously at the molecular sample is the zero-of-time (t_0). With increasing time lapse after the initiation pulse, the transient species undergoes a population change (*indicated by the growth of the red filled units at the expense of the blue filled circles*) and a structural change (*shown as the transformation of red circles into red squares*). The Diffraction-Difference Method dramatically enhances the significance of the transient species contribution in the diffraction-difference patterns; $I_{Scat}(t; t_{ref}; s)$. The small residual contribution of unreacted parents is not shown here.

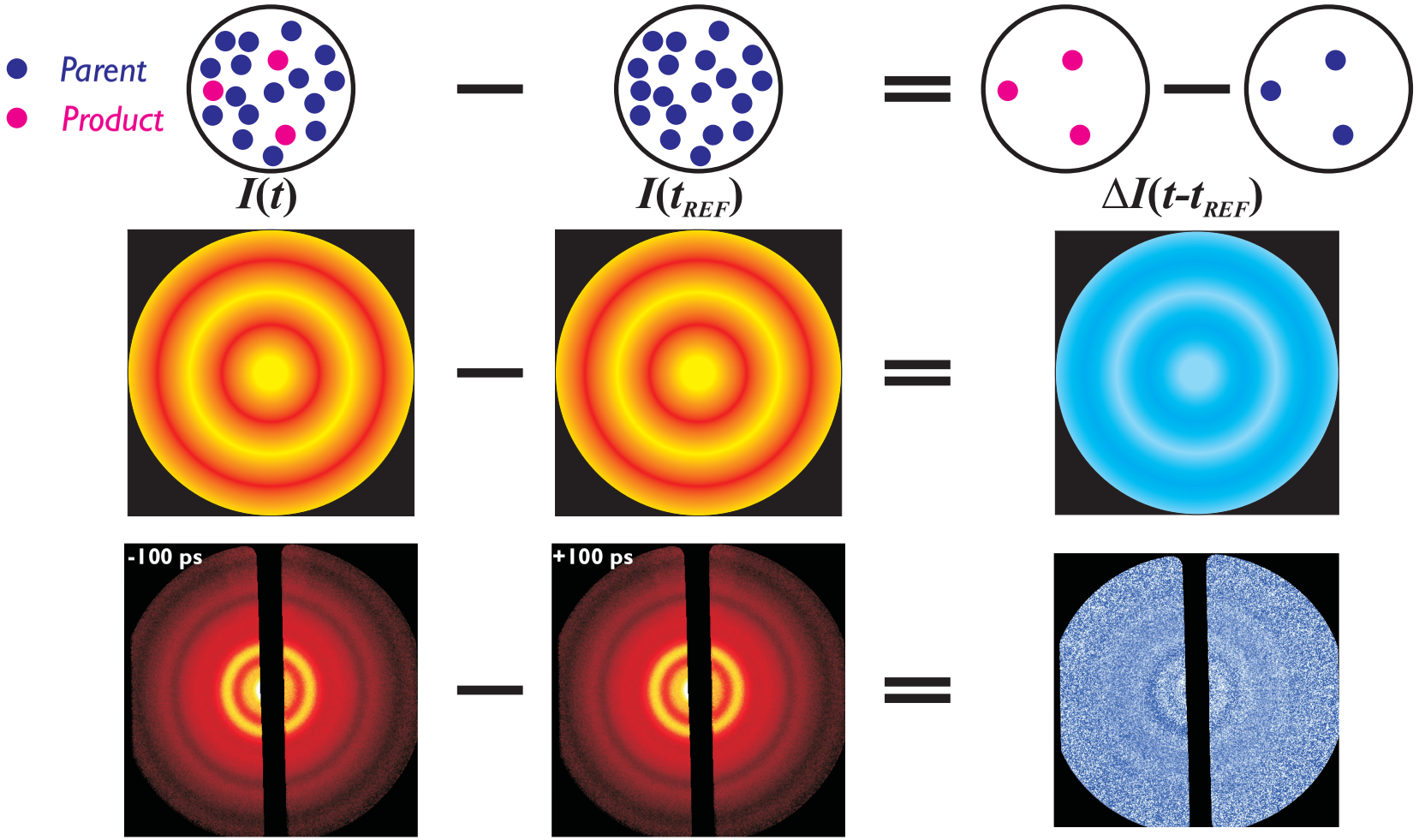

Figure 2-2. The diffraction-difference method. (*Top*) The difference of each time-resolved diffraction pattern from a reference pattern, t_{ref}, (chosen at negative or at positive time), allows the extraction of the small population of time-evolving structures embedded in the large background signal of unreacted parents. (*Middle*) Note that this dramatically enhances the significance of the transient species contribution in the diffraction-difference patterns. (*Bottom*) The time-resolved patterns of pyridine at –100 ps and +100 ps are nearly identical; however their difference reveals the diffraction signature of the transient structure.

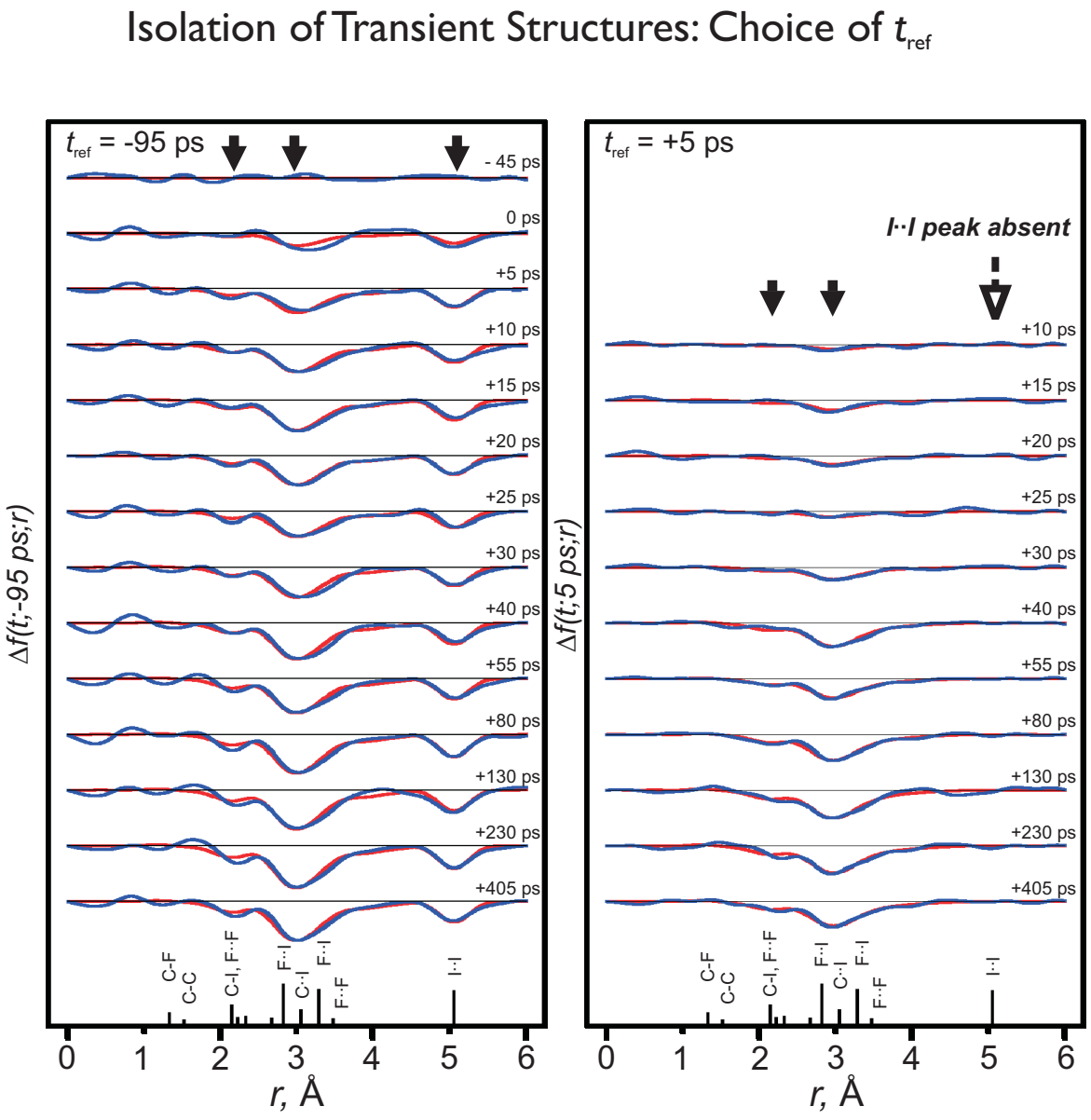

Figure 2-3. Isolation of transient species through choice of t_{ref}. Blue experimental *f(t*; *-95 ps*; *r)* curves (*left*) and *f(t*; *5 ps*; *r)* curves (*right*) obtained at varying time delays with subsequent Fourier filtering (the Fourier cutoff was 9 Å); theoretical curves are shown in red. Note that the negative peak at ~5 Å is absent in the difference curves referenced to +5 ps. Internuclear distances of the ground state *anti* conformer are indicated below the two panels for reference.

References

1. Hargittai, I.; Hargittai, M., *Stereochemical Applications Of Gas-Phase Electron Diffraction*. VCH: New York, 1988.
2. Williamson, J. C. Ultrafast Gas-Phase Electron Diffraction. Ph.D. Thesis, California Institute of Technology, Pasadena, 1998.
3. Yates, A. C., *Phys. Rev.* **1968,** *176*, 173.
4. Wilson, A. J. C.; Prince, E., *International Tables for Crystallography*. 2nd. ed.; Kluwer Academic Press: Dordrecht, 1999.
5. Ihee, H.; Cao, J.; Zewail, A. H., *Chem. Phys. Lett.* **1997,** *281*, 10.